J|A|C|S
ARTICLES
Published on Web 11/08/2002

Hydrogen Bond Vibrations of 2-Aminopyridine·2-Pyridone, a Watson−Crick Analogue of Adenine·Uracil

Andreas Müller, Francis Talbot, and Samuel Leutwyler*

Contribution from the Departement für Chemie und Biochemie, Universität Bern, Freiestrasse 3, CH-3000 Bern 9, Switzerland

Received July 19, 2002

Abstract: The 2-aminopyridine·2-pyridone complex (2AP·2PY) is linked by antiparallel N−H···O═C and N−H···N hydrogen bonds, providing a model for the Watson−Crick hydrogen bond configuration of the adenine−thymine and adenine−uracil nucleobase pairs. Mass-selected $S_1 \leftrightarrow S_0$ vibronic spectra of the supersonically cooled 2AP·2PY base pair analogue were measured by laser resonant two-photon ionization and emission spectroscopies. The hydrogen bond vibrations ν_2 (buckle, out-of-plane) and the three in-plane vibrations ν_3 (opening), ν_5 (shear), and ν_6 (stretch) were observed in the S_0 and S_1 states, giving detailed information on the stretching and deformation force constants of the (amide)N−H···N(pyridine) and the (amino)N−H···O═C hydrogen bonds. Density functional calculations with the B3LYP functional and the 6-311++G(*d,p*) and 6-311++G(*2d,2p*) basis sets yield ground-state hydrogen bond frequencies in close agreement with experiment.

1. Introduction

Although hydrogen bonds are among the weakest chemical interactions, they occupy a key position in biochemistry and biology. Antiparallel amino N−H···O═C and amide N−H···N hydrogen bonds are generic molecular recognition and structure-determining motifs in nucleic acid base pairs,[1,2] occurring in the adenine·thymine (A·T), adenine·uracil (A·U), and guanine·cytosine (G·C) base pairs in DNA and RNA, respectively. They form the basis of the molecular recognition processes on which the genetic code is based and are partly responsible for the interstrand binding and stabilization of DNA and the different types of RNA.

Accurate knowledge of the low-frequency hydrogen bond vibrations of nucleobase pairs are indispensable for deriving the basic parameters of the intermolecular interactions, such as the force constants of the "propeller-twist", "buckle", "stagger", "shear", "opening", and "stretch" intermolecular angles, distances, and motions between nucleobases.[3−6] They can be used to calibrate the atom−atom or group−group parameters which are employed in empirical force-field calculations[7,8] for molecular modeling and dynamical studies of oligonucleotides and DNA. The collective vibrational modes of DNA[4−6] have been investigated by neutron scattering and Raman spectroscopy, but these low-frequency vibrations are often masked by solvent Rayleigh and Raman scattering as well as collective modes of the DNA backbone; assignments are often difficult.[9,10] The dimerization enthalpies, entropies, and free energies of nucleobases cannot be accurately calculated without knowledge of the correct intermolecular vibrational frequencies, since these dominate the vibrational partition function and thereby the values of $\Delta_{dim}H°$, $\Delta_{dim}S°$, and $\Delta_{dim}G°$.[11]

Ab initio theoretical calculations have been performed for the doubly hydrogen bonded A·T and A·U base pairs in the gas phase using Hartree−Fock, MP2, and density functional methods, which all predict planar geometries and binding energies in the range $D_e = 10.5-13.0$ kcal/mol.[11−17] The gas-phase base pairing enthalpy for A·T was determined by mass spectrometry as $\Delta_{dim}H°_{298} = -13.0$ kcal/mol.[18] When large basis sets are employed, the Watson−Crick and Hoogsteen configurations of gas-phase A·T and A·U are nearly degenerate; on the basis of the expected existence of up to four different H bonding isomers, ab initio calculations suggest a correction of +0.9 kcal/mol to the experimental $\Delta_{dim}H°_{298}$.[12] The influence of the local solvent surrounding has also been theoretically studied by including from two to seven water molecules.[16,17]

* Address correspondence to this author. E-mail: leutwyler@iac.unibe.ch.

(1) Saenger, W. *Principles of Nucleic Acid Structures;* Springer: Berlin, 1984.
(2) Jeffrey, G. A.; Saenger, W. *Hydrogen Bonding in Biological Structures;* Springer: Berlin, 1991.
(3) Dickerson, R. E.; et al. *EMBO J.* **1989**, *8*, 1−4.
(4) Chen, Y. Z.; Prohofsky, E. W. *J. Chem. Phys.* **1984**, *80*, 6291.
(5) Chen, Y. Z.; Prohofsky, E. W. *J. Chem. Phys.* **1991**, *94*, 4665.
(6) Cocco, S.; Monasson, R. *J. Chem. Phys.* **2000**, *112*, 10017.
(7) MacKerell, A. D., Jr.; et al. *J. Phys. Chem. B* **1998**, *102*, 3586.
(8) Cieplak, P. In *The Encyclopedia of Computational Chemistry*; v. R. Schleyer, P., Allinger, N. L., Clark, T., Gasteiger, J., Kollman, P. A., Schaefer, H. F., III, Schreiner, P. R., Eds.; John Wiley: Chichester, U.K., 1998.
(9) Urabe, H.; Hayashi, H.; Tominaga, Y.; Nishimura, Y.; Kubota, K.; Tsuboi, M. *J. Chem. Phys.* **1985**, *82*, 531.
(10) Urabe, H.; Sugawara, Y.; Tsukakoshi, M.; Kasuya, T. *J. Chem. Phys.* **1991**, *95*, 5519.
(11) Špirko, V.; Šponer, J.; Hobza, P. *J. Chem. Phys.* **1997**, *106*, 1472.
(12) Brameld, K.; Dasgupta, S.; Goddard, W. A., III. *J. Phys. Chem. B* **1997**, *101*, 4851.
(13) Šponer, J.; Leszczynski, J.; Hobza, P. *J. Chem. Phys.* **1996**, *100*, 1965.
(14) Kratochvil, M.; Engkvist, O.; Sponer, J.; Jungwirth, P.; Hobza, P. *J. Phys. Chem. A* **1998**, *102*, 6921.
(15) Bertran, J.; Oliva, A.; Rodriguez-Santiago, L.; Sodupe, M. *J. Am. Chem. Soc.* **1998**, *120*, 8159.
(16) Zhanpeisov, N. U.; Leszczynski, J. *J. Phys. Chem. A* **1998**, *102*, 6167.
(17) Guerra, C. F.; Bickelhaupt, F. M. *Angew. Chem., Int. Ed* **1999**, *38*, 2942.
(18) Yanson, I. K.; Teplitzky, A. B.; Sukhodub, L. F. *Biopolymers* **1979**, *18*, 1149.

10.1021/ja0209969 CCC: $22.00

UV spectroscopic investigations of the Watson−Crick interactions of two isolated nucleobases face several problems: the first is the large number of hydrogen bonded dimer structures that become possible when the chemical bonding constraints operative in the biological environment are removed. Even if H bonding through the N9−H group of the purine and N1−H of the pyrimidine bases is eliminated (as in nucleosides and nucleotides), there remain many possibilities to form two H bonds between adenine and uracil (or thymine) besides the Watson−Crick configuration.[19,20] The second is that the Watson−Crick H bonding configuration may not be the most stable gas-phase isomer, as predicted by theory for A·T and A·U, see earlier.[12,13] The third problem is that the pyrimidine nucleic acid bases are difficult to investigate by electronic spectroscopic methods, because of their rapid ($\approx 10^{12}$ s^{-1}) nonradiative deactivation of the S_1 and higher excited electronic states,[21,22,23] broad absorption bands, and near-total absence of fluorescence, even at low temperature or in supersonic jets.[24−26] Using laser resonant two-photon ionization (R2PI), narrow-band UV spectra have recently been measured for the supersonic jet-cooled purines guanine (G), adenine (A), and several methylated derivatives,[19,27−30] and for the guanosine nucleoside.[31] The intermolecular vibrations of the guanine·guanine (G·G) and guanine·cytosine (G·C) nucleobase dimers have been observed by Nir et al. for the S_1 excited state.[20,32−34] However, no gas-phase spectra have so far been obtained for the A·T or A·U nucleobase dimers in the gas phase.

To circumvent these problems, we investigated the pyridine-based nucleobase analogues 2-aminopyridine (2AP)[35−41] and 2-pyridone (2PY),[42−44] which both exhibit narrow-band absorption and fluorescence spectra in the gas phase. 2AP and 2PY present the same hydrogen bonding sites as adenine and uracil (or thymine), respectively, as in Figure 1.

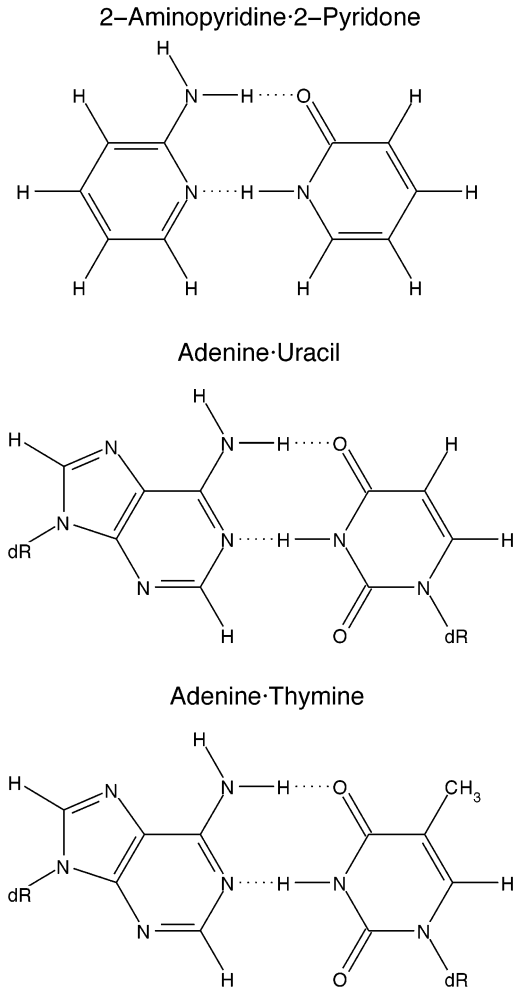

Figure 1. Comparison of the 2-aminopyridine·2-pyridone (2AP·2PY) complex with the Watson−Crick configurations of the adenine·uracil and adenine·thymine base pairs, showing the close analogy of the hydrogen bond patterns.

On the other hand, 2AP and 2PY lack the other hydrogen bond donor/acceptor groups of the canonical nucleic acid bases and can *only* hydrogen bond via the (amino)N−H···O═C and (amide)N−H···N(pyridine) hydrogen bonds, analogous to the Watson−Crick configurations of A·T and A·U. Both the 2AP[35−41] and 2PY[42−44] monomers have been extensively studied using high-resolution gas-phase spectroscopic techniques and are known to fluoresce with moderate quantum yields.

Using laser resonant two-photon ionization and fluorescence spectroscopies at vibronic resolution, we measured the low-frequency intermolecular vibrational frequencies of 2AP·2PY in the S_0 and S_1 electronic states in supersonic jets. These give direct information on the N−H···N and N−H···O hydrogen bonds, their stretching and deformation force constants, as well as indirect information on the hydrogen bond dissociation energy. The measurements are complemented by ab initio density functional calculations. We and others have recently shown that DFT methods are suitable for the treatment of H bonded base complexes and their analogues.[17,45−49] Specifically,

(19) Nir, E.; Janzen, C.; Imhof, P.; Kleinermanns, K.; de Vries, M. S. *J. Chem. Phys.* **2001**, *115*, 4604.
(20) Nir, E.; Janzen, C.; Imhof, P.; Kleinermanns, K.; de Vries, M. S. *Phys. Chem. Chem. Phys.* **2002**, *4*, 740.
(21) Lamola, A. A.; Eisinger, J. *Biochim. Biophys. Acta* **1971**, *240*, 313.
(22) Daniels, M.; Hauswirth, W. *Science* **1971**, *171*, 675.
(23) Callis, P. R. *Annu. Rev. Phys. Chem.* **1983**, *34*, 329.
(24) Fujii, M.; Tamura, T.; Mikami, N.; Ito, M. *Chem. Phys. Lett.* **1986**, *126*, 583.
(25) Tsuchiya, Y.; Tamura, T.; Fujii, M.; Ito, M. *J. Phys. Chem.* **1988**, *92*, 1760.
(26) Brady, B. B.; Peteanu, L. A.; Levy, D. H. *Chem. Phys. Lett.* **1988**, *147*, 538.
(27) Nir, E.; Brauer, B.; Grace, L.; de Vries, M. S. *J. Am. Chem. Soc.* **1999**, *121*, 4896.
(28) Kim, N. J.; Jeong, G.; Kim, Y. S.; Sung, J.; Kim, S. K.; Park, Y. D. *J. Chem. Phys.* **2000**, *113*, 10051.
(29) Lührs, D.; Viallon, J.; Fischer, I. *Phys. Chem. Chem. Phys.* **2001**, *3*, 1827.
(30) Plützer, C.; Nir, E.; de Vries, M. S.; Kleinermanns, K. *Phys. Chem. Chem. Phys.* **2001**, *3*, 5466.
(31) Nir, E.; Imhof, P.; Kleinermanns, K.; de Vries, M. S. *J. Am. Chem. Soc.* **2000**, *122*, 8091.
(32) Nir, E.; Imhof, P.; Kleinermanns, K.; de Vries, M. S. *Nature (London)* **2000**, *408*, 949.
(33) Nir, E.; Janzen, C.; Imhof, P.; Kleinermanns, K.; de Vries, M. S. *Phys. Chem. Chem. Phys.* **2002**, *4*, 732.
(34) Nir, E.; Müller, M.; Grace, L. I.; de Vries, M. S. *Chem. Phys. Lett.* **2002**, *355*, 59.
(35) Kydd, R. A.; Mills, I. *J. Mol. Struct.* **1972**, *42*, 320.
(36) Hollas, J. M.; Kirby, G. H.; Wright, R. A. *Mol. Phys.* **1970**, *18*, 327.
(37) Hollas, J. M.; Musa, H.; Ridley, T. *J. Mol. Struct.* **1984**, *104*, 107.
(38) Wallace, S. *J. Phys. Chem.* **1985**, *86*, 2218.
(39) Hager, J.; Wallace, S. *J. Phys. Chem.* **1985**, *89*, 3833−3841.
(40) Hager, J.; Ivanco, M.; Smith, M. A.; Wallace, S. *Chem. Phys.* **1985**, *105*, 397.
(41) Borst, D. R.; Roscioli, J. R.; Pratt, D. W. *J. Phys. Chem. A* **2002**, *106*, 4022.
(42) Nimlos, M. R.; Kelley, D. F.; Bernstein, E. R. *J. Phys. Chem.* **1989**, *93*, 643.
(43) Held, A.; Champagne, B. B.; Pratt, D. *J. Chem. Phys.* **1991**, *95*, 8732.
(44) Hatherley, L. D.; Brown, R. D.; Godfrey, P. D.; Pierlot, A. P.; Caminati, W.; Damiani, D.; Melandri, S.; Favero, L. B. G. *J. Phys. Chem.* **1993**, *97*, 46.
(45) Guerra, C. F.; Bickelhaupt, F. M.; Snijders, J. G.; Baerends, E. J. *J. Am. Chem. Soc.* **2000**, *122*, 4117.
(46) Gu, J.; Leszczynski, J. *J. Phys. Chem. A* **2000**, *104*, 1898.

we demonstrated for the (2-pyridone)$_2$ complex, which is an H bonding analogue of the uracil·uracil self-dimer,[47] that the B3LYP/6-311++G(*d,p*) method yields very good agreement with the experimental gas-phase N−H···O hydrogen bond distance[50,51] and all six intermolecular vibrational frequencies.[47,49]

2. Methods

2.1. Computational Procedure. Minimum-energy structures were first calculated at the SCF level using the 6-31G(*d,p*) basis set, followed by optimizations with the B3LYP functional and the valence triple-ζ 6-311++G(*d,p*) and 6-311++G(*2d,2p*) basis sets, which include diffuse and one or two sets of polarization functions. All optimizations were performed without symmetry restrictions, resulting in slightly nonplanar structures for both 2-aminopyridine and 2-aminopyridine·2-pyridone. To obtain very accurate electronic energies, the root-mean-square (RMS) difference between the density matrix elements in consecutive cycles of the procedure was required to be $< 1 \times 10^{-10}$ and structures were optimized until the largest component of the nuclear gradient was 2×10^{-6} hartree/bohr or hartree/rad. Normal coordinate calculations were carried out at the minimum-energy geometries. The SCF *intra*molecular harmonic frequencies were scaled by a factor of 0.9277, determined by least-squares fitting to strong intramolecular fundamentals of the (2-pyridone)$_2$ dimer, (2PY)$_2$,[47] to account for the overestimate of vibrational frequencies at the SCF level. The SCF *inter*molecular vibrational frequencies and *all* DFT frequencies remained unscaled. All calculations were performed using the GAUSSIAN 94 and 98 programs.[52]

2.2. Experimental Methods. 2AP·2PY complexes were synthesized and cooled in a 20 Hz pulsed supersonic expansion. Helium or neon carrier gas at ~1.5 bar backing pressure was passed through a container containing 2AP (Aldrich) heated to 315 K and then through the pulsed nozzle (0.4 mm diameter) containing the 2-hydroxypyridine (Aldrich). For the two-color resonant two-photon ionization (2C-R2PI) and the UV hole-burning measurements, the nozzle was heated to 340 K. For the fluorescence spectra, higher temperatures (345−355 K) and a larger nozzle (0.6 mm) were employed to increase the absolute concentration of the dimer in the supersonic jet.

2C-R2PI spectra were measured by crossing the skimmed beam with overlapping excitation and ionization laser beams inside the source of a linear time-of-flight mass spectrometer. Excitation was performed with the frequency-doubled UV output of a pulsed DCM dye laser, pumped by a frequency-doubled Nd/YAG laser. The excitation intensity was kept very low, <10 kW/cm^2 (<50 μJ/pulse), to avoid optical saturation effects. For the ionization step, the 10 times more intense (500 μJ/pulse) frequency-quadrupled output of the same Nd/YAG laser was employed, which was fully spatially and temporally overlapped with the excitation pulse. For UV spectral hole-burning (HB) measurements, a second independently tunable frequency-doubled DCM dye laser with an even higher pulse energy (850 μJ/pulse) was used. This was pumped by a second Nd/YAG laser, which was fired 160 ns before the first and synchronized by a Stanford DG535 digital delay unit. The HB laser beam was spatially overlapped with the excitation and ionization laser beams.

For the dispersed fluorescence experiments, the UV laser beam (500 μJ/pulse) crossed the jet 20 mm from the nozzle. The emitted fluorescence was collected using a combination of a spherical mirror and quartz optics and dispersed with a SOPRA F1500 UHRS 1.5 m monochromator; the spectral band-pass was 4−5 cm^{-1}. The dispersed fluorescence light was either detected by a cooled Hamamatsu R928 photomultiplier or by an LN_2 cooled 27 × 8 mm^2 back-thinned UV-enhanced CCD array with 15 × 15 μm^2 pixels (Princeton Instruments). Dependent on signal intensity, spectra were accumulated between 20 min to 1 h. Other experimental details are as given previously.[47−49]

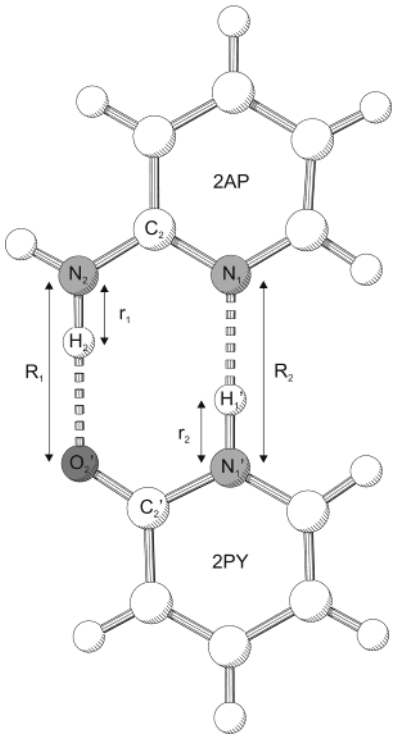

Figure 2. Ab initio calculated minimum-energy structure of the 2-aminopyridine·2-pyridone nucleobase analogue pair, at the B3LYP/6-311++G(*2d,2p*) level.

3. Results and Interpretation

3.1. Ab Initio Results. The B3LYP/6-311++G(*2d,2p*) optimized structure of 2AP·2PY is shown in Figure 2. At both the SCF and density functional levels, the 2PY complex is calculated to be nonplanar: the "propeller-twist" displacement of the dimer can be characterized by the torsional angle $\tau_1(C_2-N_1\cdots N_1'-C_2') = +6.1°$, or by $\tau_2(C_6-N_1\cdots N_1'-C_6') = -8.4°$ (the atom labels of 2PY are primed). Also, the amino group is slightly nonplanar, characterized by the torsional angle $\tau_3(N_2-C_2-C_3-C_4) = 0.7°$. By contrast, the minimum-energy structure of the A·U nucleobase dimer is calculated to be completely planar with the B3LYP/6-311++G(*d,p*) method/basis-set combination.

The two hydrogen bond distances are quite different: the B3LYP/6-311++G(*2d,2p*) calculation predicts the $N_2\cdots O_2'$ distance to be $R_1 = 2.88$ Å and the $N_1\cdots N_1'$ distance as $R_2 = 2.94$ Å; cf. Figure 2 also. At the SCF/6-31G(*d,p*) level, the corresponding distances are ≈ 0.14 Å longer. For the (2-pyridone)$_2$ dimer, the SCF/6-31G(*d,p*) method was clearly shown to give hydrogen bonds which are much too long and hence rotational constants which are too small.[47,49]

The six intermolecular modes derive from the three rotational and three translational degrees of freedom and can be qualitatively separated into three out-of-plane and three approximately in-plane vibrations.[11,13,47,53] The intermolecular harmonic frequencies calculated at the B3LYP/6-311++G(*d,p*) and B3LYP/

(47) Müller, A.; Talbot, F.; Leutwyler, S. *J. Chem. Phys.* **2000**, *112*, 3717.
(48) Müller, A.; Talbot, F.; Leutwyler, S. *J. Chem. Phys.* **2001**, *115*, 5192.
(49) Müller, A.; Talbot, F.; Leutwyler, S. *J. Chem. Phys.* **2002**, *116*, 2836.
(50) Held, A.; Pratt, D. *J. Am. Chem. Soc.* **1990**, *112*, 8629.
(51) Held, A.; Pratt, D. *J. Chem. Phys.* **1992**, *96*, 4869.
(52) Frisch, M. J.; Trucks, G. W.; Schlegel, H. B.; et al. *GAUSSIAN 98*, revision A.11.A; Gaussian, Inc.: Pittsburgh, PA, 1998.
(53) Florian, J.; Leszczynski, J.; Johnson, B. G. *J. Mol. Spec.* **1995**, *349*, 421.

Table 1. Ab Initio SCF/6-31G(*d,p*), B3LYP/6-311++G(*d,p*), and B3LYP/6-311++G(*2d,2p*) Harmonic Frequencies and Experimental S_0 and S_1 State Frequencies (cm^{-1}) of the Intermolecular Vibrations of the 2-Aminopyridine·2-Pyridone Complex[a]

		SCF	B3LYP		experiment	
mode	description	6-31G(*d,p*)	6-311++G(*d,p*)	6-311++G(*2d,2p*)	S_0	S_1
ν_1	propeller-twist	22.2	22.7	22.6		20.9
ν_2	buckle	36.9	34.9	36.7	35.1	42.6
ν_3	opening	68.8	79.3	78.3	82.2	76.9
ν_4	stagger	83.3	84.1	84.9		
ν_5	shear	103.3	113.8	112.5	103.3	98.5
ν_6	stretch	122.0	139.3	136.2	136.3	126.4
RMS deviation (cm^{-1})		9.84	5.65	5.06		

[a] Intramolecular SCF frequencies (italic) are scaled by 0.92 769; all DFT frequencies are unscaled.

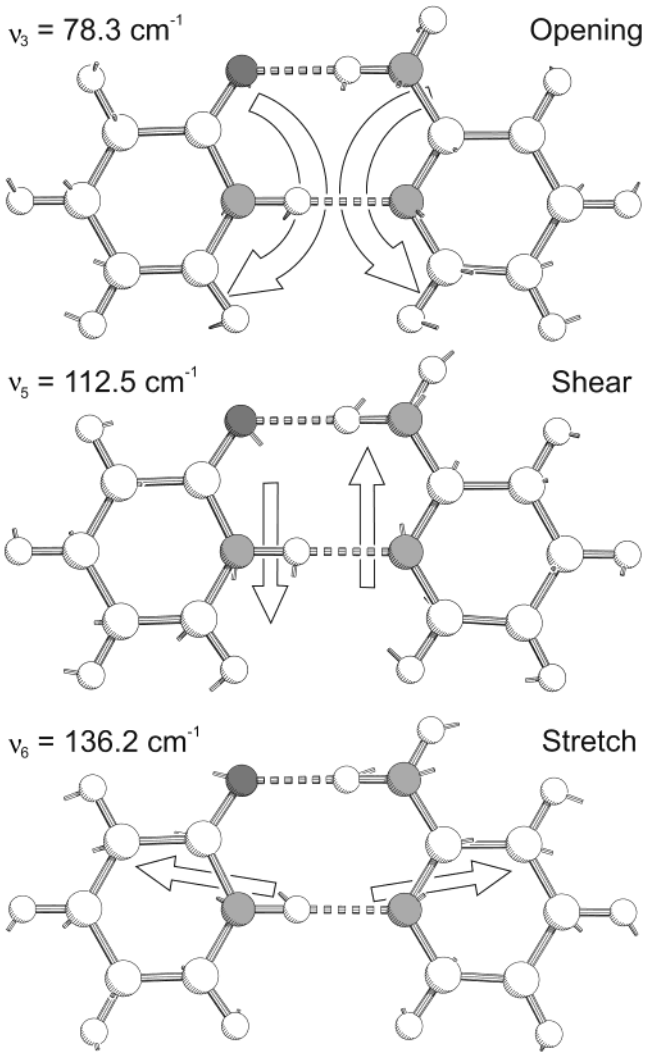

Figure 3. In-plane normal-mode eigenvectors ν_3, ν_5, and ν_6 of 2-aminopyridine·2-pyridone, with B3LYP/6-311++G(*2d,2p*) harmonic frequencies; see also text and Table 1.

6-311++G(*2d,2p*) levels are collected in Table 1 and are compared to experiment below. The intermolecular in-plane (*ip*) vibrational eigenvectors are shown in Figure 3; note that we use the coordinate definitions of Dickerson et al.:[3] ν_3 is the H bond "opening" mode and ν_5 the "shearing" mode, which derive from the dis- and conrotatory motions of each monomer, respectively. The H bond stretching vibration ν_6 derives from translational motions along the long in-plane axis of the complex. The out-of-plane modes are ν_1, corresponding to the "propeller-twist" deformation, ν_2, the "buckle" deformation, and ν_4, the "stagger" mode; see Figure 4.

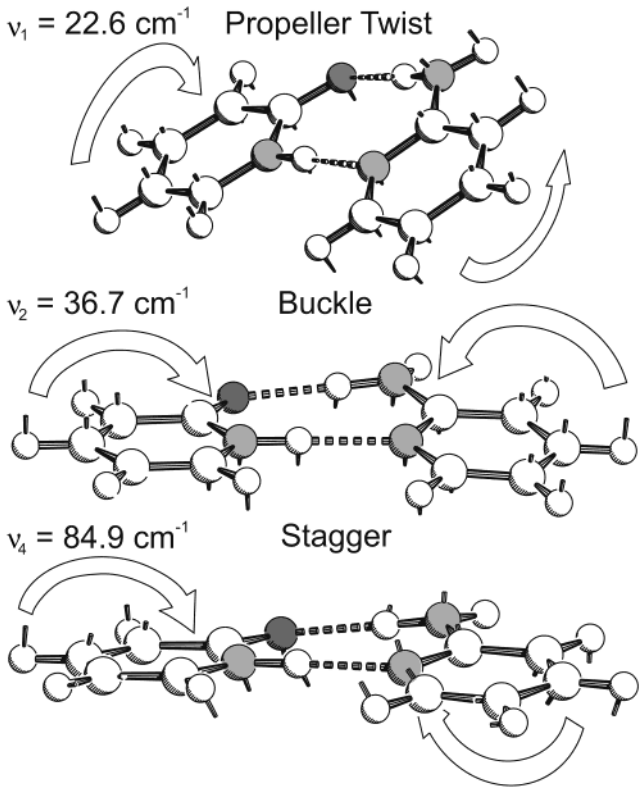

Figure 4. Out-of-plane normal-mode eigenvectors ν_1, ν_2, and ν_4 of 2-aminopyridine·2-pyridone, with B3LYP/6-311++G(*2d,2p*) harmonic frequencies; see also text and Table 1.

3.2. Resonant Two-Photon Ionization Spectra. We measured two-color resonant two-photon ionization spectra of 2AP·2PY over the 30 000−31 200 cm^{-1} range. This electronic transition corresponds essentially to the $S_1 \leftarrow S_0$ absorption of 2-pyridone, which is perturbed as a result of the interaction with the 2-aminopyridine moiety. The first 300 cm^{-1} of the spectrum are shown in Figure 5. The intense band at 32 066.2 cm^{-1} is assigned as the $S_1 \leftarrow S_0$ electronic origin; it lies ≈400 cm^{-1} to the blue of the electronic origin of 2PY.[50,51] The S_1 state intermolecular vibrational excitations of 2AP·2PY in Figure 5 are marked by their frequencies relative to the origin; the most intense bands lie at 0_0^0 + 77, + 98, and + 126 cm^{-1}. The vibronic band frequencies, assignments, and intensities relative to the 0_0^0 band are listed in Table 1 and will be discussed following the interpretation of the fluorescence spectra. The $S_1 \leftarrow S_0$ transition of the 2-aminopyridine moiety lies some 3000 cm^{-1} higher,[37−40] in a spectral region not investigated in this work.

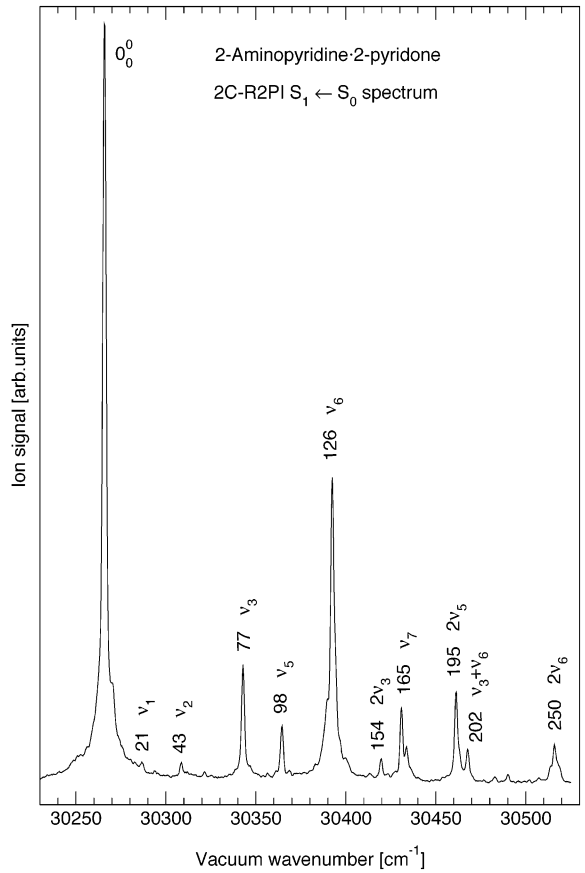

Figure 5. Two-color resonant two-photon ionization spectrum of 2-aminopyridine·2-pyridone in the vicinity of the $S_1 \leftarrow S_0$ electronic absorption. The S_1 state vibrational excitations are labeled both by the mode(s) (cf. Table 1) and by the frequency relative to the origin.

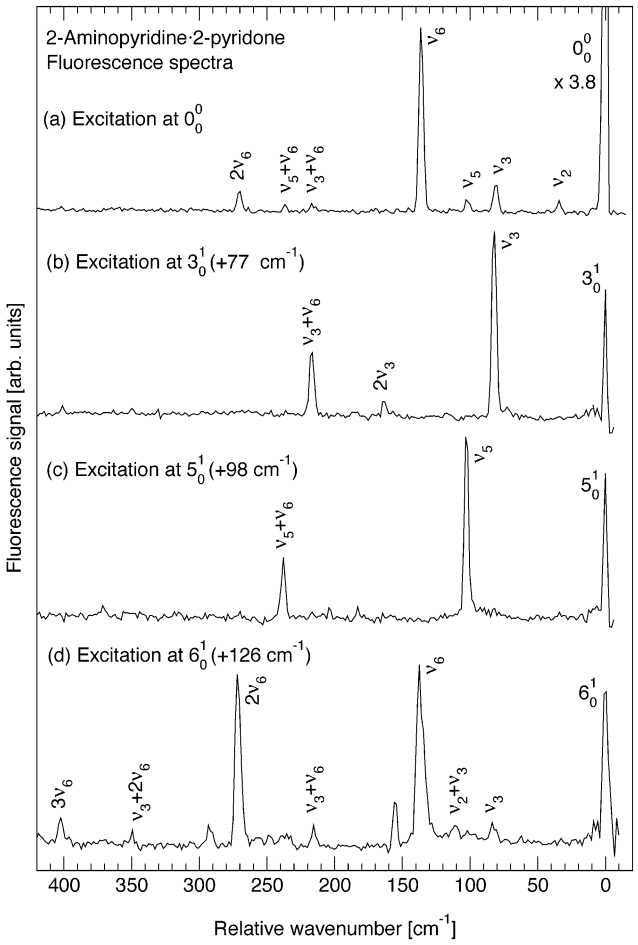

Figure 6. Dispersed fluorescence emission spectra of 2-aminopyridine·2-pyridone, excited at (a) the 0_0^0 band at 30 266.2 cm^{-1}, (b) the $0_0^0 + 77$ cm^{-1} band, (c) the $0_0^0 + 98$ cm^{-1} band, and (d) the $0_0^0 + 126$ cm^{-1} band. The monochromator band-pass was 4 cm^{-1}. The frequency scale is relative to the respective excitation frequency.

UV−UV hole-burning experiments were also performed in order to identify possible isomers of the 2AP·2PY complex. When the hole-burning laser was tuned to the 0_0^0 band, *all* bands in Figure 5 were depleted by ∼70%. This identifies the entire spectrum shown in Figure 5 as originating from excitations out of the 2AP·2PY vibrationless ground state.

The $S_1 \leftarrow S_0$ spectrum of 2AP·2PY is shifted 400−500 cm^{-1} to lower frequencies with respect to the spectra of other dimers formed in the expansion, that is, the 2-hydroxypyridine·2-pyridone dimer (2HP·2PY) and the $(2PY)_2$ dimer, whose electronic origins lie at 30 655.7 cm^{-1} and 30 766.3 cm^{-1}, respectively. Although both species have masses which are 1 amu lower than that of 2AP·2PY and can be cleanly separated in the time-of-flight mass spectrometer, the ^{13}C isotopomers of both species coincide with the mass of 2AP·2PY. Since the concentration of $(2PY)_2$ is 2−5 times higher than that of 2AP·2PY, noticeable contributions to the R2PI spectrum of 2AP·2PY arise from $(2PY)_2-^{13}$C for frequencies above 30 766 cm^{-1}.[47−49]

In neon supersonic expansions at high backing pressures and late delay times in the nozzle pulse, an additional weak band is observed at 30 286 cm^{-1}, blue shifted by 18.1 cm^{-1} relative to the 2AP·2PY electronic origin. This band is attributed to the electronic origin of the 2AP·2PY·Ne complex, which fragments upon ionization using 266 nm photons. The assignment was verified by the absence of this band when using helium carrier gas, as in the spectrum shown in Figure 5. For $(2PY)_2$ and 2HP·2PY, the analogous Ne complexes were also observed with origins blue shifted by 19−22 cm^{-1} relative to the 0_0^0 bands of the dimers.[47−49]

3.3. Dispersed Fluorescence Spectra and Ground-State Vibrations. Dispersed fluorescence spectra of 2AP·2PY were measured by excitation at the electronic origin and at the $0_0^0 +$ 77, + 98, and + 126 cm^{-1} bands, as indicated in Figure 6. We note that the fluorescence spectrum of bare 2-pyridone is devoid of vibrational bands up to 440 cm^{-1}.[42] At low frequencies, three weak intermolecular vibrational fundamentals are observed in Figure 6a: the band at 35.1 cm^{-1} is assigned as the ν_2'' buckle vibration, since it lies very close to the B3LYP/6-311++G-(*2d,2p*) calculated frequency 36.7 cm^{-1}.

The next weak band at 82.2 cm^{-1} is assigned as the ν_3'' opening vibration, predicted at 78.3 cm^{-1}. An alternative assignment is as the ν_4'' "stagger" vibration, calculated to lie at 84.9 cm^{-1}. However, the $S_1 \leftrightarrow S_0$ electronic transition dipole moment lies in the plane of the 2-pyridone molecule, which enhances in-plane vibrations of the dimer, favoring the assignment as ν_3''. The band observed at 103.3 cm^{-1} is assigned as the ν_5'' "shearing" vibration; the calculated frequency is 112.5 cm^{-1}. The strongest band in Figure 6a at 136.3 cm^{-1} is assigned to the H bond stretch ν_6'', in excellent agreement with the calculated frequency, 136.2 cm^{-1}. The $2\nu_6''$ overtone is observed

Table 2. 2-Aminopyridine·2-Pyridone Experimental Ground-State Intermolecular Vibrational Frequencies (cm^{-1}, Relative to the Respective Excitation Frequency)

	frequency[a]			
assignment	0_0^0(100[a])	3_0^1	5_0^1	6_0^1
ν_2''	35.1 (1.1)			
ν_3''	82.2 (3.9)	82 (100[a])		82 (13)
$\nu_2'' + \nu_3''$				111 (8)
ν_5''	103.3 (1.7)		103 (100[a])	
ν_6''	136.3 (26.9)			136 (100[a])
$2\nu_4''/\nu_6'' + \nu_1''$?				155 (25)
$2\nu_3''$		164 (9)		
$\nu_3'' + \nu_5''$			181 (7)	
$\nu_3'' + \nu_6''$	217 (3.1)	217 (35)		217 (14)
$\nu_5'' + \nu_6''$	237 (0.7)		237 (34)	
$2\nu_6''$	270 (2.5)			270 (95)
$2\nu_4'' + \nu_6/2\nu_6'' + \nu_1''$?				292 (15)
$\nu_3'' + 2\nu_6''$				350 (12)
$3\nu_6''$				402 (16)

[a] Intensity of most intense band = 100. Intensities are in parentheses.

at 270.0 cm^{-1}, and a weak excitation at 216.5 cm^{-1} is attributed to the $\nu_4'' + \nu_6''$ combination.

As shown in Figure 6b, laser excitation at the $0_0^0 + 77$ cm^{-1} band strongly enhances the transition at 82.2 cm^{-1}, assigned to the ν_3'' opening mode. The $2\nu_3''$ overtone of the opening mode is also weakly observed. The stretching fundamental is not observed at all, but a medium strong band at 258.8 cm^{-1} can be assigned as the $\nu_3'' + \nu_6''$ combination band. Laser excitation at the $0_0^0 + 98$ cm^{-1} band, shown in Figure 6c, leads to a strong enhancement of the 103.3 cm^{-1} band, assigned as the ν_5'' shearing vibration. Similar to the emission spectrum in Figure 6b, the stretching fundamental is not observed; the strong band at 258.8 cm^{-1} is assigned as the $\nu_3'' + \nu_6''$ combination band. The large Franck−Condon factors to modes involving ν_5'' imply that the excited-state vibration is ν_5'. Excitation at the $0_0^0 + 126$ cm^{-1} band, Figure 6d, leads to a three-membered progression in ν_6'' with bands at 136.3, 270.0, and 402.2 cm^{-1}. This implies that the excitation is dominantly to the hydrogen bond stretching vibration ν_6'. By combining the fundamental and two overtone frequencies, we can determine the diagonal anharmonicity, giving the harmonic frequency $\omega_e = 138.1$ cm^{-1} and anharmonicity constant $\omega_e x_e = 1.03$ cm^{-1}. The complete set of the S_0 state vibrational assignments is given in Table 2.

3.4. Fluorescence Lifetime. The fluorescence decay time of 2AP·2PY was measured to be $\tau_{fl} = 14 \pm 1$ ns at the electronic origin at 30 266.2 cm^{-1}. This value is slightly longer than that of bare 2-pyridone, $\tau_{fl} = 11 \pm 1$ ns at 29 832 (or 29 935) cm^{-1}.[43] The lifetime of bare 2-aminopyridine at its electronic origin at 33 471 cm^{-1} was measured using LIF by Hager and Wallace[39] as $\tau_{fl} = 2$ ns and recently via the Lorentzian width of the rovibronic lines by Borst et al.[41] as $\tau_{fl} = 1.5$ ns.

3.5. Excited-State Vibrations. On the basis of the enhancements of ground-state vibrations in the fluorescence spectra, discussed above, the 2C−R2PI band at $0_0^0 + 77$ cm^{-1} can be clearly assigned as the S_1 state ν_3' opening fundamental, the band at $0_0^0 + 98$ cm^{-1} as the ν_5' shearing fundamental and the band at $0_0^0 + 126$ cm^{-1} as the ν_6' stretching fundamental; cf. also Figure 5. These three S_1 state frequencies are lower than the corresponding S_0 state intermolecular vibrational frequencies, by 6%, 5%, and 7%, respectively.

The 2C-R2PI band at +21 cm^{-1} is tentatively assigned to the excited-state propeller-twist fundamental ν_1'; the only other candidate for such a low vibrational frequency is the ν_2' buckle vibration, but this is assigned to another band (see later). Furthermore a weak band at +56.8 cm^{-1} can then be assigned as the first overtone $2\nu_1'$. The R2PI band at +43 cm^{-1} is tentatively assigned to the excited-state buckle fundamental ν_2'. We have not been able to measure fluorescence spectra from any of these three very weak excitations with sufficient signal/noise ratio. If the assignments are correct, they imply that the S_1 state ν_1' and ν_2' frequencies increase by ~20% relative to the ground state (calculated or observed) frequencies. If the 2AP·2PY complex is nonplanar, as calculated for the ground state, then transitions in out-of-plane fundamentals are allowed. Since the $S_1 \leftrightarrow S_0$ transition dipole moment lies within the plane of the 2-pyridone moiety, the out-of-plane vibrational excitations should not be intense, as observed.

Should further work show that the complex is planar in both electronic states, then the assignments of ν_1' and ν_2' would have to be revised to $2\nu_1'$ and $2\nu_2'$. This would imply a lowering of these two frequencies upon electronic excitation, which would also be in agreement with the observed spectral blue shift and the lowering of the in-plane frequencies.

3.6. Discussion. 3.6.1. Bond Strength and Vibrational Frequency Changes upon Electronic Excitation. When the so-called "A" electronic origin[42,50,51] of 2PY is chosen as a point of reference, the spectral shift of the electronic origin of 2AP·2PY is +435.4 cm^{-1} toward higher frequency. This translates to a 1.24 kcal/mol *decrease* of the hydrogen bond dissociation energy D_0 upon $S_1 \leftarrow S_0$ electronic excitation. For the analogous 2HP·2PY complex[48] and for the 2-pyridone dimer,[47,49−51] the spectral shifts are +825 cm^{-1} and +926 cm^{-1}, respectively, thus also to the blue, but approximately twice as large.

In agreement with the decrease of hydrogen bond strength, the intermolecular vibrational frequencies of the three in-plane modes ν_3 (opening), ν_5 (shear), and ν_6 (stretch) decrease by 5−7% upon electronic excitation. Interestingly, however, the out-of-plane buckle frequency ν_2 increases from 35 to 43 cm^{-1}, if the abovementioned assignment is correct. The ν_2 vibrational eigenvector shows some involvement of the inversion motion of the $-NH_2$ group of the 2-aminopyridine moiety, and the frequency increase may hence be due to a change of the amino group inversion potential in the S_1 excited state.

3.6.2. Hydrogen Bond Stretching Force Constants. The H bond stretching force constant f_σ'' of 2AP·2PY can be quantified using the ν_6'' frequency. Using the pseudodiatomic approximation,[54−56] we modeled the 2-aminopyridine and 2-pyridone molecules as pseudoatoms of masses 94.1 and 95.1 amu and the intermolecular motion as a pure one-dimensional stretching motion. The ground-state harmonic force constant is calculated to be $f_\sigma'' = 51.8$ N/m or 25.9 N/m per H bond. However, the (amino)N−H···O=C and (amide)N−H···N hydrogen bonds of 2AP·2PY must be of unequal strength. For the analogous 2-hydroxypyridine·2-pyridone dimer, 2HP·2PY, the ν_6'' stretching vibrational force constant is larger, being 70.0 N/m or an average of 35.0 N/m per H bond.[48] Since both dimers have the (amide)N−H···N(pyridine) hydrogen bond in common, the difference can be attributed to the other H bond. Thus, the

(54) Legon, A. C.; Millen, D. J. *Faraday Discuss. Chem. Soc.* **1982**, *73*, 71.
(55) Legon, A. C.; Millen, D. J. *Chem. Rev.* **1986**, *86*, 635.
(56) Legon, A. C.; Millen, D. J. *Acc. Chem. Res.* **1987**, *20*, 39.

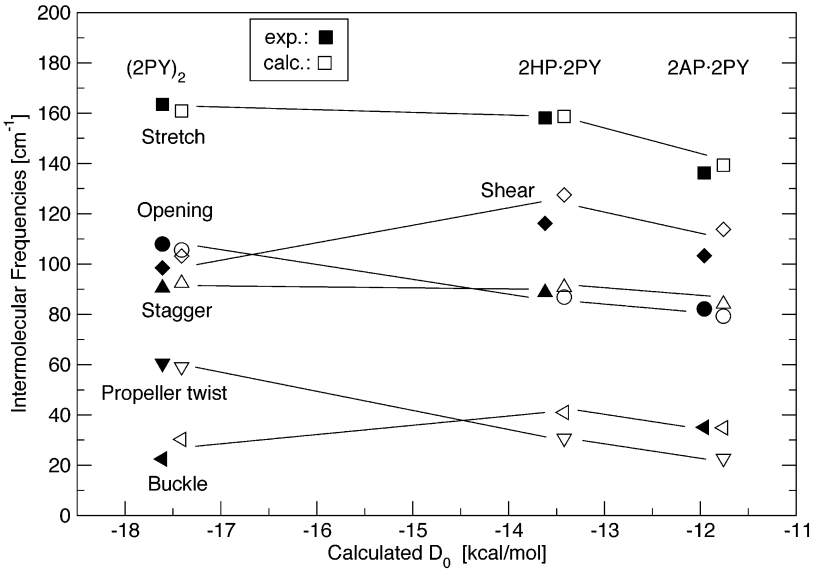

Figure 7. Comparison of the experimental and calculated S_0 state intermolecular vibrational frequencies (in cm^{-1}) of the doubly hydrogen bonded nucleobase-pair analogues $(2\text{-pyridone})_2$, 2-hydroxypyridine·2-pyridone (2HP·2PY) and 2-aminopyridine·2-pyridone (2AP·2PY) plotted vs. the calculated dissociation energies D_0, in kcal/mol. All calculations at the B3LYP/6-311++G(*d*,*p*) level.

(amino)N−H···O═C hydrogen bond of 2AP·2PY is seen to be considerably weaker than the O−H···O═C hydrogen bond of 2HP·2PY.

If we assume (i) that the additivity of stretching force constants holds for both complexes and (ii) that for 2HP·2PY the stretching force constant is equally due to both H bonds, this leads to force constants of 35 N/m for the (amide)N−H···N(pyridine) hydrogen bonds of 2HP·2PY and of 2AP·2PY and for the O−H···O═C H bond of 2HP·2PY. These values are very large and close to the stretching force constant of 37.3 N/m for the (amide)N−H···O═C hydrogen bonds of $(2PY)_2$.[47] On the other hand, these assumptions result in a lower force constant of 17 N/m for the (amino)N−H···O═C hydrogen bond of 2AP·2PY. This is in the range of "normal" values for hydrogen bond stretching force constants, which are typically 10−20 N/m.[54−56]

3.6.3. Geometry and Force Constant Change upon Electronic Excitation. The Franck−Condon factor (FCF) of the 6_1^0 band relative to the electronic origin is 27%; thus, the coupling of the ν_6 stretch to the $S_1 \leftrightarrow S_0$ electronic transition is moderate. The FCFs of the other five intermolecular vibrations are 10 times or more smaller, indicating that the geometry changes along the other intermolecular coordinates are negligible. We derived the relative displacement of the S_0 and S_1 state H bond stretching potentials, modeled as Morse potentials, from the ratios of FCFs observed in fluorescence, $I(0_0^0):I(6_1^0):I(6_2^0) = 100:26.9:2.5$. The anharmonic stretching wave functions were calculated from the 1-D vibrational Schrödinger equation corresponding to the pseudodiatomic model with the reduced mass as earlier, followed by numerical quadrature to give the Franck−Condon factors for the two transitions. The relative displacement of the potentials along the stretching coordinate is plus or minus 0.039(5) Å.

Since the $S_1 \leftarrow S_0$ electronic excitation leads to a decrease of the hydrogen bond dissociation energy by 1.24 kcal/mol, we interpret the displacement as an *increase* of the intermolecular distance by +0.039(5) Å. This parallels the $S_1 \leftarrow S_0$ increase of the intermolecular distance of +0.057(5) Å derived for the 2-pyridone dimer, $(2PY)_2$[49] (note, however, that an increase in N···O hydrogen bond distance of +0.100(5) Å was derived by Held and Pratt[51]). For the tautomeric 2HP·2PY, the analogous FCF analysis yielded an $S_1 \leftarrow S_0$ increase of the intermolecular distance of +0.079(5)Å.[48]

Using again the pseudodiatomic approximation and the same masses, we derive from the H bond stretching frequency $\nu_6' = 126.4\ cm^{-1}$ the excited-state stretching force constant $f_\sigma' = 44.5$ N/m. This is a decrease by 14% compared to the ground-state stretching force constant $f_\sigma'' = 51.8$ N/m.

3.6.4. Comparison to Density Functional Theory. The experimental determination of four out of the six intermolecular vibrational frequencies of 2AP·2PY allows for the comparison of different ab initio theoretical models. The B3LYP exchange−correlation functional combined with basis sets including polarization and diffuse functions have been shown to perform well for the prediction of the vibrational frequencies as well as for the structure and rotational constants of the $(2PY)_2$ dimer.[47,49] As Table 1 shows, the B3LYP/6-311++G(*d*,*p*) and 6-311++G(*2d*,*2p*) frequencies for the ν_2'' (buckle), ν_3'' (opening), and ν_6'' (stretching) vibrations are very close to experiment; only for ν_5'', the predictions are 9% too high.

In contrast, at the SCF/6-31G(*d*,*p*) level, the ν_2'', ν_3'', and ν_6'' vibrational frequencies differ quite substantially from experiment. The overall performance of the models can be gauged from the root-mean-square deviation of the calculated from the observed frequencies, $\Delta\nu(RMS)$, which clearly favors the two B3LYP calculations.

3.6.5. Comparison to Vibrational Frequencies of Other Nucleobase Analogues. We also compared the experimental and calculated intermolecular vibrational frequencies of 2AP·2PY with those determined earlier for the 2HP·2PY and $(2PY)_2$ complexes. Figure 7 shows the measured intermolecular fundamental frequencies (full symbols) and the B3LYP/6-311++G(*d*,*p*) calculated harmonic frequencies (open symbols), plotted versus the B3LYP/6-311++G(*d*,*p*) calculated dissociation energies D_0. First, we note that the overall agreement between the 13 intermolecular vibrational fundamental frequencies observed

Table 3. A Comparison of the B3LYP/6-311++G(*d,p*) Calculated Intermolecular Binding Energies, D_e, Dissociation Energies, D_0, and Vibrational Frequencies of 2-Aminopyridine·2-Pyridone and Adenine·Uracil

	energy (kcal/mol)	
	2-aminopyridine·2-pyridone	adenine·uracil
D_e	−13.55	−12.85
BSSE[a]	0.62	0.74
$D_e^{CPC_b}$	−12.93	−12.11
D_0	−11.96	−10.85
intermolecular vibrations (cm^{-1})		
ν_1 (propeller-twist)	22.7	33.1
ν_2 (buckle)	34.9	24.4
ν_3 (opening)	79.3	60.0
ν_4 (stagger)	84.1	64.9
ν_5 (shear)	113.8	102.2
ν_6 (stretch)	139.3	118.0

[a] Basis set superposition error. [b] Counterpoise-corrected binding energy.

so far and the corresponding B3LYP calculated harmonic frequencies is very good. The exceptions are the shear frequencies of 2HP·2PY and 2AP·2PY, which the B3LYP calculation overestimates by 10%. Second, there is a linear correlation between the vibrational frequency and the dissociation energy for the opening and propeller-twist frequencies. Third, the decrease in dissociation energy does *not* systematically correlate with a decrease of vibrational frequency: thus, the stagger frequencies remain nearly independent of the dissociation energy, and the shear and buckle frequencies go through a maximum for 2HP·2PY.

3.6.6. Comparison of 2-Aminopyridine·2-Pyridone to Adenine·Uracil and Guanine·Cytosine. Obviously, the electronic structure of the purine·pyrimidine dimers are somewhat different from the pyridine·pyridone system of the analogue, and the question arises as to how well 2AP·2PY really models its nucleobase dimer counterparts A·T and A·U. Since no experimental data are so far available for gas-phase A·T or A·U, we compared the calculated binding energies, dissociation energies, intermolecular frequencies, and force constants of 2AP·2PY to those of adenine·uracil, at the B3LYP/6-311++G*(d,p)* level. The structure optimization of A·U was performed using the same criteria as for 2AP·2PY; see section 2.1. The results are compared in Table 3. The binding energy D_e of adenine·uracil is calculated to be −12.85 kcal/mol, which is 0.70 kcal/mol or 5% lower than that for 2AP·2PY. The predicted dissociation energy of adenine·uracil is −10.85 kcal/mol, about 1.1 kcal/mol or 9% smaller than that of 2AP·2PY. Thus, the D_es and D_0s are roughly comparable; astonishingly, the larger purine−pyrimidine system, which is more polarizable and would be expected to have larger dispersive and inductive stabilizing contributions to the H bonds, is calculated to be slightly less strongly bound than the 2AP·2PY model dimer.

With the exception of the propeller-twist frequency, all the intermolecular frequencies of adenine·uracil are lower than those of 2AP·2PY. Most of this effect can be ascribed to the larger masses of adenine and uracil relative to 2-aminopyridine and 2-pyridone, respectively. A revealing comparison is that between force constants:[57] The pseudodiatomic H bond stretching force constants derived from the B3LYP/6-311++G*(d,p)* calculations are f_σ = 54.1 N/m for 2AP·2PY and 50.3 N/m for adenine·uracil. The 7% smaller H bond stretching force constant of adenine·uracil is in good agreement with the 10% smaller dissociation energy.

Another interesting comparison can be made with respect to the jet-cooled guanine·cytosine (G·C) dimer spectra that Nir et al. observed[32] and recently interpreted.[33] From the analysis of the N−H and O−H stretching vibrations in their IR−UV hole-burning spectrum,[33] they concluded that the G·C species observed has three hydrogen bonds and involves guanine in the normal *keto*, 9H form, but cytosine in the nonbiological *trans-enol* form; see also the scheme below.[33]

2−Aminopyridine·2−Pyridone

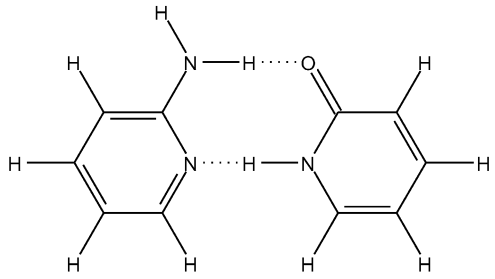

Guanine·Cytosine (K9−E1 isomer)

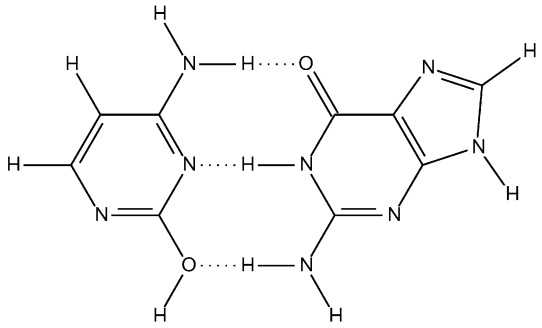

This so-called K9-E1 structure is only the third most stable form; the two more strongly bound keto−keto G·C isomers were not observed.[33] The S_1 excited state is also less strongly bound than the ground state, in this case by 1.3 kcal/mol.

From the one-color R2PI $S_1 \leftarrow S_0$ spectra, they assigned the S_1 state ν_6' stretching frequency of the K9-E1 G·C isomer as 120 cm^{-1}. In the pseudodiatomic approximation, this gives a S_1 state stretching force constant f_σ' = 54.3 N/m, which is 22% larger than the S_1 state force constant f_σ' = 44.5 N/m derived above for 2AP·2PY. As shown in the scheme, the (amino)N−H···O═C and (amide)N−H···N hydrogen bonds of the K9-E1 G·C isomer and of 2AP·2PY are of the same type and relative orientation. If for the moment the differences in electronic structure between the monomers are disregarded (2-aminopyridine vs cytosine and 2-pyridone vs guanine), it appears that the (amino)N−H···O−H hydrogen bond in this G·C isomer yields does not yield as large a stabilization as the other two H bonds.

(57) The force constants given in the normal-mode analysis outputs of Gaussian98 are not suitable for comparison between different molecules or even different isotopomers of the same molecule. They result from an arbitrary normalization of the Cartesian normal-mode eigenvector to 1, thereby resulting in "force constants" which are mass-dependent; cf. www.Gaussian.com/vib.htm.

4. Conclusions

2-Aminopyridine·2-pyridone is a hydrogen bonding analogue of the adenine·uracil and adenine·thymine nucleic acid base pairs. Using mass-selective laser spectroscopic methods, the fundamental frequencies of four hydrogen bond vibrations were measured in the S_0 state and of five in the S_1 state. These were assigned to the hydrogen bond vibrations ν_1 (propeller-twist, S_1 state only), ν_2 (buckle), ν_3 (opening), ν_5 (shear), and ν_6 (stretch).

Upon $S_1 \leftarrow S_0$ excitation, the ν_3, ν_5, and ν_6 vibrational frequencies decrease by 5−7% and the hydrogen bond dissociation energy D_0 by 1.24 kcal/mol. A very similar decrease in dissociation energy upon electronic excitation was recently observed for the K9-E1 isomer of guanine·cytosine.[33] Although there are significant differences in the excited-state level structure of 2-pyridone compared to uracil or thymine, analogous weakening of the interstrand hydrogen bonds upon photoexcitation may be expected following the $\pi-\pi^*$ excitations of the pyrimidine and purine nucleobases, and this may destabilize the nucleic acid.

The harmonic stretching force constant of 2AP·2PY was determined as $f_\sigma = 25.9$ N/m per hydrogen bond, averaged over both H bonds. For the analogous 2-hydroxypyridine·2-pyridone dimer, 2HP·2PY, the average stretching vibrational force constant is substantially larger, 35.0 N/m per H bond.[48] Assuming that additivity of stretching force constants holds for both complexes and that the force constant of 2HP·2PY is equally due to both H bonds implies a force constant of only 17 N/m for the (amino)N−H···O═C hydrogen bond of 2AP·2PY. This is within the range of the 10−20 N/m measured for "normal" hydrogen bonds.[54−56] By the same reasoning, the stretching force constant of the (amide)N−H···N(pyridine) hydrogen bond of 2AP·2PY is 35 N/m, double that of the (amino)N−H···O═C hydrogen bond, and close to the 37.3 N/m measured for the (amide)N−H···O═C hydrogen bonds of $(2PY)_2$.[49] This implies that the H bond stretching force constants in these nucleobase dimer analogues can far exceed those of normal hydrogen bonds. More detailed information, including the possible role of resonance-assisted hydrogen bonding, will be obtained from studies involving 2-pyridone and single hydrogen bond acceptors.

The quantum-chemical calculations provide data on geometrical, vibrational, and binding energy properties of 2AP·2PY. As shown previously for other nucleobase dimer analogues,[47,48] the B3LYP density functional combined with the 6-311++G(*d,p*) and 6-311++G(*2d,2p*) basis sets predicts very good ground-state intermolecular vibrational frequencies: the ν_2'', ν_3'', and ν_6'' predicted frequencies are within a few percent of the observed fundamentals. Only the frequency of the ν_5'' shear mode is somewhat overestimated, as seen previously for the 2HP·2PY dimer.[48] The SCF 6-31G(*d,p*) method underestimates the hydrogen bond strength, as seen from the calculated ν_3'' and ν_6'' frequencies, which are 16 and 11% lower than experiment, and from the calculated N···O and N···N hydrogen bond distances, which are ∼0.14 Å longer than those calculated by the B3LYP density functional method.

With respect to the biologically important interactions between nucleic acid bases, both the experimental intermolecular stretching force constants as well as the calculated interaction and dissociation energies imply that the two H bonds of $(2\text{-pyridone})_2$, which is a model for the uracil dimer (U·U),[47] are ≈ 50% stronger than those of 2-aminopyridine·2-pyridone, which models gas-phase A·U (or A·T).

Acknowledgment. This work was supported by the Schweiz. Nationalfonds (Project No. 20-53932.98 and 2000-61890). The calculations were partly carried out at the Centro Svizzero di Calcolo Scientifico (CSCS) in Manno, Switzerland.

JA0209969